a0005

Point-Vortex Dynamics

S Boatto, IMPA, Rio de Janeiro, Brazil
D Crowdy, Imperial College, London, UK

s0005

Introduction

p0005 Vortices have a long fascinating history. Descartes wrote in his *Le Monde*:

> ...que tous les mouvements qui se font au Monde sont en quelque façon circulaire: c'est à dire que, quand un corps quitte sa place, il entre toujours en celle d'un autre, et celui-ci en celle d'un autre, et ainsi de suite jusques au dernier, qui occupe au même instant le lieu délaissé par le premier.

p0010 In particular, Descartes thought of vortices to model the dynamics of the solar system, as reported by W W R Ball (1940) bib0020:

> Descartes' physical theory of the universe, embodying most of the results contained in his earlier and unpublished *Le Monde*, is given in his *Principia*, 1644,... He assumes that the matter of the universe must be in motion, and that the motion must result in a number of vortices. He stated that the sun is the center of an immense whirlpool of this matter, in which the planets float and are swept round like straws in a whirlpool of water.

p0015 Descartes' theory was later on recused by Newton in his *Principia* in 1687. Few centuries later, W Thomson (1867) bib0195 the later Lord Kelvin, made use of vortices to formulate his atomic theory: each atom was assumed to be made up of vortices in a sort of ideal fluid. In 1878–79 the American physicist A M Mayer conducted a few experiments with needle magnets placed on floating pieces of cork in an applied magnetic field, as toy models for studying atomic interactions and forms (Mayer 1878 bib0135 bib0140 bib0145 bib0150 bib0155, Aref *et al.* 2003 bib0010). In 1883 inspired by Mayer experiments, J J Thomson combined W Thomson's atomic theory with H von Helmholtz's point-vortex theory (Helmholtz 1858 bib0050): he thought as the electrons were point vortices inside a positively charged shell (see **Figure 1**), the vortices being located at the vertices of regular parallelograms and investigated about the stability of such structures (see Thomson (1883, section 2.1) bib0200). The vortex-atomic theory survived for quite a few years up to Rutherford's experiments proved that atoms have quite a different structure! Before continuing this historical/modeling overview, let's address the following question:

> what is a vortex and, more specifically, what is a point-vortex?

p0020 Roughly speaking, following Descartes, a vortex is an entity which makes particles move along circular-like orbits. Examples are the cyclones and anticyclones in the atmosphere, (see **Figure 2**). Mathematically speaking, let $\boldsymbol{u} = (u, v, w) \in \mathbb{R}^3$ be a velocity field, the associated vorticity field ω is defined to be

$$\omega = \nabla \wedge \boldsymbol{u} \qquad [1]$$

In this article we are considering exclusively inviscid flows which are also incompressible, that is,

$$\nabla \cdot \boldsymbol{u} = 0 \qquad [2]$$

and have constant density ρ, which we normalize to be equal to 1 ($\rho = 1$). In two dimensions, a point-vortex field is the simplest of all vorticity fields: it can be thought as an entity where the vorticity field is concentrated into a point. In other words, point vortices are singularities of the vorticity field! Then, in the plane the vorticity field associated to a system of N point vortices is

$$\omega(\boldsymbol{r}) = \sum_{\alpha=1}^{N} \Gamma_\alpha \delta(\boldsymbol{r} - \boldsymbol{r}_\alpha) \qquad [3]$$

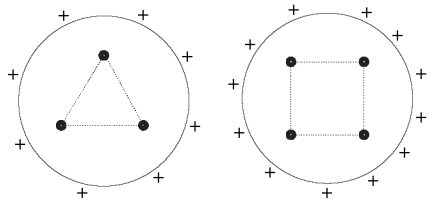

AU2

f0005 **Figure 1** Thomson atomic model: (a) atom with three electrons and (b) atom with four electrons. From Thomson JJ (1883) *A Treatise on the Motion of Vortex Rings*. New York: Macmillan and Thomson JJ (1904) *Electricity and Matter* Westminster Archibald Constable.

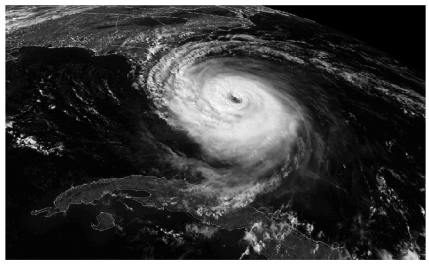

f0010 **Figure 2** Hurricane Jeanne. Reproduced with permission from the National Oceanic and Atmospheric Administration (NOAA) (www.noaanews.noaa.gov).

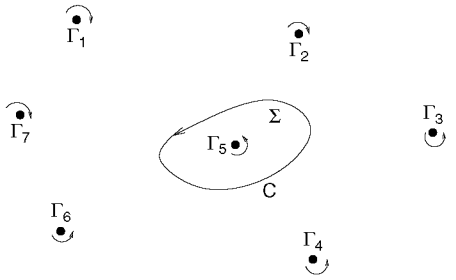

AU3 f0015 **Figure 3**

where $\Gamma_\alpha, \alpha = 1, \ldots, N$, is a constant and corresponds to the vorticity (or circulation) of the α-vortex, situated at $\boldsymbol{r}_\alpha$. In fact by definition, the circulation around a curve C delimiting a region Σ with boundary C,

$$\Gamma_C = \oint_C \boldsymbol{u} \cdot \mathrm{d}\boldsymbol{s} = \iint_\Sigma (\nabla \wedge \boldsymbol{u}) \cdot \boldsymbol{n}\, \mathrm{d}A = \iint_\Sigma \omega \quad [4]$$

where we have used Stokes' theorem to bring in the vorticity. Then if the region contains only the αth point vortex, we obtain

$$\Gamma_C = \iint_\Sigma \omega \cdot \mathrm{d}\boldsymbol{A} = \Gamma_\alpha \quad [5]$$

by eqn [3]. A positive (resp. negative) sign of Γ_α indicates that the corresponding point vortex induces an anticlockwise (resp. clockwise) particle motion, see **Figure 4a**)). Is there an analog of a point-vortex system for a three-dimensional flow?

p0025 Yes, and this brings in the analogy between vortex lines and magnetic field lines that Mayer used in his experiments with floating magnets. In fact, in three dimensions, the notion of a point vortex can be extended to that one of a straight vortex line (see **Figure 4b**), where, by definition, a vortex line is a curve that is tangent to the vorticity vector ω at each of its point. In this context we would like to mention the beautiful experiments of Yarmchuck–Gordon–Packard on vortices in superfluid helium. They observed the formation of stable polygonal configurations of identical vortices, quite similar to the ones observed by Mayer with his magnets (see **Figures 5** and **1**).

p0030 One would like to understand how such configurations form and to give a theoretical account about their stability. In order to answer these questions we have to first be able to describe the dynamics of a system of point vortices from a mathematical point of view.

Evolution Equations

s0010

p0035 Can point vortices be viewed as "discrete" (or localized) solutions of Euler equation in two dimensions? Let us consider the Euler equation

$$\frac{\partial \boldsymbol{u}}{\partial t} + \boldsymbol{u} \cdot \nabla \boldsymbol{u} = -\nabla p + \boldsymbol{f} \quad [6]$$

where p is the pressure, $\boldsymbol{f} = -\nabla U$ is a conservative force, and restrict our attention to the two-dimensional setting, for example, vortex dynamics on the plane (or a sphere). Then it is immediate that by taking the curl of eqn [6] we obtain the evolution equation of the vorticity, that is,

$$\frac{\partial \omega}{\partial t} + \boldsymbol{u} \cdot \nabla \omega = 0, \quad \text{or} \quad \frac{D\omega}{Dt} = 0 \quad [7]$$

where the operator $D/Dt = \partial/\partial t + \boldsymbol{u} \cdot \nabla$ is called the material derivative and describes the evolution along the flow lines. It follows from eqn [7] that in two dimensions the vorticity is conserved as it is transported along the flow lines. Then a natural question arises: supposing the vorticity field ω is known, is it possible to deduce the velocity field $\boldsymbol{u}$ generating ω? Or in other words, is it possible to solve the system of eqns [1]–[2]? It is immediate to see that in general the solution is not unique, if some boundary conditions are not specified (see bib0125 Marchioro and Pulvirenti (1993)). Furthermore, as bib0025 already observed by Kirchhoff in 1876 (Boatto and Cabral 2003), in two dimensions we can recast the fluid equations [1]–[2] into a Hamiltonian formalism. In fact, notice that on the plane $\boldsymbol{u} = (\dot{x}, \dot{y})$ and eqn [2] is still satisfied if we represent the velocity components as

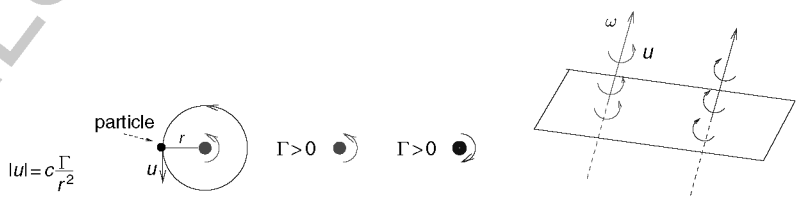

f0020 **Figure 4** (a) Advected by the velocity field of one point vortex, a test particle follows a circular orbit, with a speed proportional to the absolute value of the vortex circulation and inversely proportional to the square of its distance from the vortex. (b) Straight vortex lines.

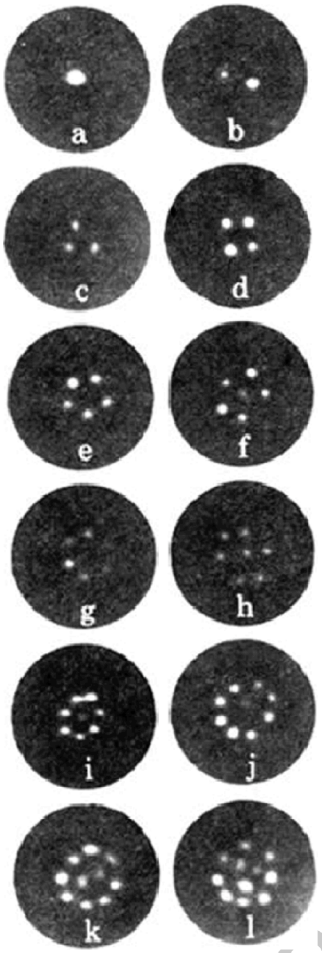

f0025 **Figure 5** Photographs of vortex configurations in a rotated sample of superfluid helium with 1,...,11 vorticies. Reprinted figure with permission from Yarmchuk EJ, Gordon MJV, and Packard RE (1979) Observation of stationary vortices arrays in rotating superfluid Helium. *Physical Review Letters* 43(3): 214–217. Copyright (1979) by the American Physical Society.

$$\dot{x} = \frac{\partial \Psi}{\partial y}, \qquad \dot{y} = -\frac{\partial \Psi}{\partial x} \qquad [8]$$

that is, by means of Ψ, called the stream function. Formally, Ψ plays the rôle of a Hamiltonian for the pair of conjugate variables (x, y) and it is used to describe the dynamics of a test particle, located at (x, y) and advected by the flow. By substituting [8] into [1], we obtain

$$\Delta \Psi(\boldsymbol{r}) = \omega(\boldsymbol{r}) \qquad [9]$$

that is, a Poisson equation with ω as a source term. Then, once we specify the vorticity field, by inverting [9] we obtain the stream function Ψ to be

$$\Psi(\boldsymbol{r}) = \int G(\boldsymbol{r}, \boldsymbol{r}')\omega(\boldsymbol{r}')\, \mathrm{d}\boldsymbol{r}' \qquad [10]$$

where $G(\boldsymbol{r}, \boldsymbol{r}')$ is the Green's function, solution of the equation $\Delta G(x, y) = -\delta(x, y)$. The Green's function both for the plane and the sphere is (Marchioro and Pulvirenti 1993) bib0125

$$G(\boldsymbol{r}, \boldsymbol{r}') = -\frac{1}{4\pi} \log \|\boldsymbol{r} - \boldsymbol{r}'\|^2 \qquad [11]$$

where $\|\boldsymbol{r} - \boldsymbol{r}'\|^2 = (x - x')^2 + (y - y')^2$. By [10], once we specify the vorticity field $\omega(\boldsymbol{r})$ we can compute Ψ, and by replacing it into [8] the velocity field becomes

$$\boldsymbol{u}(\boldsymbol{r}) = \int K(\boldsymbol{r}, \boldsymbol{r}')\omega(\boldsymbol{r}')\, \mathrm{d}\boldsymbol{r}' \qquad [12]$$

where $K(\boldsymbol{r}, \boldsymbol{r}') = -(\boldsymbol{r} - \boldsymbol{r}')^{\perp}/[2\pi \|\boldsymbol{r} - \boldsymbol{r}'\|^2]$ and it represents the velocity field generated by a point vortex of intensity one, located at $\boldsymbol{r}'$. Then by considering the vorticity field generated by point vortices, eqn [3], together with eqn [11], eqn [10] becomes

$$\begin{aligned} \Psi(\boldsymbol{r}) &= -\frac{1}{4\pi} \int \log \|\boldsymbol{r} - \boldsymbol{r}'\|^2 \left(\sum_{\alpha=1}^{N} \Gamma_\alpha \delta(\boldsymbol{r}' - \boldsymbol{r}_\alpha) \right) \mathrm{d}\boldsymbol{r}' \\ &= -\frac{1}{4\pi} \sum_{\alpha=1}^{N} \Gamma_\alpha \log \|\boldsymbol{r} - \boldsymbol{r}_\alpha\|^2 \end{aligned} \qquad [13]$$

Equation [13] describes together with [8], the dynamics of a test particle at a point $\boldsymbol{r} = (x, y)$ in the plane. Analogously, it can be shown that the dynamics of a systems of point vortices in the plane is given by the equations

$$\Gamma_\alpha \frac{\mathrm{d}x_\alpha}{\mathrm{d}t} = \frac{\partial H_\nu}{\partial y_\alpha}, \qquad \Gamma_\alpha \frac{\mathrm{d}y_\alpha}{\mathrm{d}t} = -\frac{\partial H_\nu}{\partial x_\alpha} \qquad [14]$$

where $(q_\alpha, p_\alpha) = (x_\alpha, \Gamma_\alpha y_\alpha), \alpha = 1, \ldots, N$, is pair of conjugate variables and H_ν is the generalization of the stream function Ψ (eqn [13]):

$$H_\nu = -\frac{1}{4\pi} \sum_{\substack{\alpha,\beta=1 \\ \alpha \neq \beta}}^{N} \Gamma_\alpha \Gamma_\beta \log \|\boldsymbol{r}_\alpha - \boldsymbol{r}_\beta\|^2 \qquad [15]$$

Notice that the vortex Hamiltonian H_ν (eqn [15]) is an autonomous Hamiltonian and, as we will discuss in the first subsection, it provides a good Lyapunov-like function to study stability properties of some vortex configurations. Moreover, H_ν is invariant with respect to rotations and translations, then by the Noether theorem there are other first integrals of motion, that is,

$$L = \sum_{k=1}^{N} \Gamma_k \parallel \boldsymbol{x}_k \parallel^2, \qquad M_x = \sum_{k=1}^{N} \Gamma_k x_k,$$
$$M_y = \sum_{k=1}^{N} \Gamma_k y_k$$

expressing, respectively, the conservation of angular momentum, L, and linear momentum, $\boldsymbol{M} = (M_x, M_y)$, on the plane. We shall denote with M the magnitude of $\boldsymbol{M}$ (i.e., $M = \|\boldsymbol{M}\|$). Furthermore, by introducing the Poisson bracket

$$[f,g] = \sum_{\alpha=1}^{N} \left(\frac{\partial f}{\partial q_\alpha}\frac{\partial g}{\partial p_\alpha} - \frac{\partial f}{\partial p_\alpha}\frac{\partial g}{\partial q_\alpha} \right)$$
$$= \sum_{\alpha=1}^{N} \frac{1}{\Gamma_\alpha} \left(\frac{\partial f}{\partial x_\alpha}\frac{\partial g}{\partial y_\alpha} - \frac{\partial f}{\partial y_\alpha}\frac{\partial g}{\partial x_\alpha} \right)$$

we can construct three integrals in involution out of the four conserved quantities L, M_x, M_y, and H_v. These are $L, M_x^2 + M_y^2$ and H_v: in fact,

$$[H_v, L] = 0, \qquad \left[H_v, M_x^2 + M_y^2\right] = 0,$$
$$\left[L, M_x^2 + M_y^2\right] = 0$$

It is then possible to reduce the system of equations from N to $N-2$ degrees of freedom. A Hamiltonian system with N degrees of freedom is integrable whenever there are N independent integrals of motion in involution. It follows that a vortex system with $N \leq 3$ is integrable, whereas the system of equations of four identical vortices has been shown by Ziglin to be nonintegrable in the sense that there are no other first integrals analytically depending on the coordinates and circulations, and functionally independent of L, H_v, M_x, M_y (see Ziglin (1982)). The following, however, has been shown:

1. Let $K = \sum_{\alpha=1}^{N} k_\alpha$ be the total vorticity, $\boldsymbol{M} = (M_x, M_y)$ the total momentum and $M = \|\boldsymbol{M}\|$. Then, as shown by Aref and Stremler (1999), if $K = 0$ and $M = 0$, N-vortex problem [16] is integrable.

2. A system of four identical vortices (i.e., $k_\alpha = k$ for $\alpha = 1, \ldots, 4$) can undergo periodic or quasiperiodic motion for special initial conditions (see Aref and Pomphrey (1982)). More specifically, the motion of a system of four identical vortices can be periodic, quasiperiodic, or chaotic depending on the symmetry of the initial configuration. In fact, every vortex configuration that belongs to the subspace of symmetric configurations – $x_\alpha = -x_{\alpha+2}$ and $y_\alpha = y_{\alpha+2}, \alpha = 1, 2$ – gives rise to an integrable vortex motion.

p0040 We have that up to two vortices, the motion is almost always periodic and the orbits are circles; the only exception being the case for which $k_2 = -k_1$, when the circles degenerate into straight lines. Thus, a configuration of two point vortices is always a relative equilibrium configuration, that is, there exists a specific reference frame in which the two vortices are at rest. If the vortices are identical ($\Gamma_1 = \Gamma_2 = \Gamma$), the motion is synchronous with frequency $\Omega = \Gamma/\pi$ and the vortices share the same circular orbit (see **Figure 6a**). If the vortices are not identical and have vorticities of different magnitudes (say $|\Gamma_1| > |\Gamma_2|$), their motion is still synchronous and periodic, with frequency $\Omega = (\Gamma_1 + \Gamma_2)/(2\pi)$, and the vortices move on different circular orbits (with $r_2 < r_1$) both centered at the center of vorticity. Note that for both cases, identical and nonidentical vortices, we can view the vortex dynamics in a co-rotating frame where the vortices are simply at rest.

p0045 For three vortices we can have periodic and quasiperiodic motion, depending on the initial conditions, and for four vortices we can have periodic, quasiperiodic, or weakly chaotic motion.

Remarks p0050

(i) The nonintegrability of the 4-vortex system was also proved for configurations of nonidentical vortices. Koiller and Carvalho (1989) gave an analytical proof for $\Gamma_1 = -\Gamma_2$ and $\Gamma_3 = \Gamma_4 = \epsilon, 0 \ll \epsilon \ll 1$. Moreover, Castilla *et al.* (1993) considered the case: $\Gamma_1 = \Gamma_2 = \Gamma_3 = 1$ and $\Gamma_4 = \epsilon$.

(ii) Due to the translational and rotational symmetries of H_v, there are some analogies between the N-vortex problem and the N-body problem,

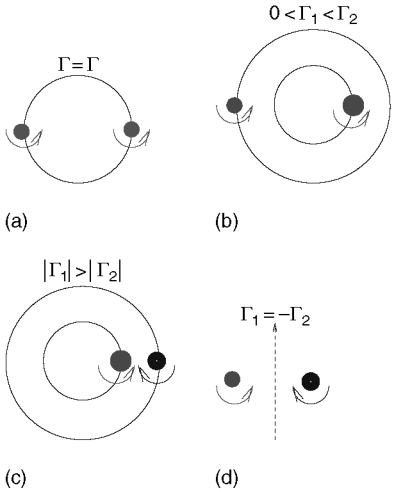

Figure 6(a–d) For $N = 2$ the vortex dipole exhibits a synchronous and the orbits are in general circular orbits, with the exception of the case (d) for which $\Gamma_1 = -\Gamma_2$ and the circular orbit degenerates into a line (or a circle of infinite radius). f0030

especially for what concerns configurations of relative equilibria (see Albouy (1996) and Glass (2000)). A relative equilibrium is a vortex (or mass) configuration that moves without change of shape or form, that is, a configuration which is steadily rotating or translating. A few examples are vortex polygons (see **Figure 7**) like the ones studied by Thomson, Mayer, Yarmchuk–Gordon–Packard, Boatto–Cabral (2003), Cabral–Schmidt (1999/
AU5 2000), Dritschel–Polvani (1993), Lim–Montaldi–Roberts (2001), Sakajo (2004). For an exhaustive review on relative equilibria of vortices, see the article by Aref *et al.* (2003). We shall discuss about stability of polygonal vortex configuration in the following subsection.

(iii) As shown by Kimura (1999) in a beautiful geometrical formalism, on the unit sphere (S^2) and on the Hyperbolic plane (H^2), the vortex Hamiltonians [15] are

$$H_v = -\frac{1}{4\pi}\sum_{\alpha\neq\beta}^{N}\Gamma_\alpha\Gamma_\beta\log(1-\cos\rho_{\alpha\beta}) \quad \text{on } S^2$$

$$H_v = -\frac{1}{4\pi}\sum_{\alpha\neq\beta}^{N}\Gamma_\alpha\Gamma_\beta\log\frac{\cosh\rho_{\alpha\beta}-1}{\cosh\rho_{\alpha\beta}+1} \quad \text{on } H^2$$

where

$$\cos\rho_{\alpha\beta} = \cos\theta_\alpha\cos\theta_\beta + \sin\theta_\alpha\sin\theta_\beta\cos(\phi_\alpha-\phi_\beta) \quad \text{on } S^2$$

$$\cosh\rho_{\alpha\beta} = \cosh\theta_\alpha\cosh\theta_\beta + \sinh\theta_\alpha\sinh\theta_\beta\cos(\phi_\alpha-\phi_\beta) \quad \text{on } H^2$$

On S^2, θ_α and ϕ_α are, respectively, the co-latitude and the longitude of the α-vortex, $\alpha = 1, \ldots, N$. We can define canonical variables q_α and p_α on S^2 and H^2, respectively, as

$$q_\alpha = \Gamma_\alpha\cos\theta_\alpha, \qquad p_\alpha = \phi_\alpha \quad \text{on } S^2$$
$$q_\alpha = \Gamma_\alpha\cosh\theta_\alpha, \qquad p_\alpha = \phi_\alpha \quad \text{on } H^2$$

Montaldi *et al.* (2002) studied vortex dynamics on a cylindrical surface, and Soulière and Tokieda AU6 (2002) considered vortex dynamics on surfaces with symmetries.

(iv) As we shall see in the section on point vortex motion, it is sometimes useful to employ the complex analysis formalism. Then the variables of interest are $z_\alpha = x_\alpha + iy_\alpha, \alpha = 1, \ldots, N$, and its conjugate $\bar{z}_\alpha$, the Hamiltonian [15] takes the form

$$H_v = -\frac{1}{2\pi}\sum_{\alpha\neq\beta}\Gamma_\alpha\Gamma_\beta\log|z_\alpha - z_\beta|$$

and the equations of motions become

$$\dot{z}_\alpha = \frac{i}{2\pi}\sum_{\beta\neq\alpha,\beta=1}^{N}\Gamma_\beta\frac{z_\alpha - z_\beta}{|z_\alpha - z_\beta|^2}, \quad \alpha = 1, \ldots, N \quad [16]$$

(v) Equation [14] can we rewritten in a more compact form as

$$\frac{dX}{dt} = J\nabla_X H_v \quad [17]$$

where

$$X = (q_1, \ldots, q_N, p_1, \ldots, p_N)$$
$$\nabla_X = \left(\frac{\partial}{\partial q_1}, \ldots, \frac{\partial}{\partial q_N}, \frac{\partial}{\partial p_1}, \ldots, \frac{\partial}{\partial p_N}\right)$$
$$J = \begin{pmatrix} O & \mathbb{I} \\ -\mathbb{I} & O \end{pmatrix}$$

$\mathbb{I}$ being the $N \times N$ identity matrix.

(vi) How close is the point-vortex model to the original Euler equation? Point-vortex systems represent discrete solutions of the Euler equation in a "weak" sense – see both the book and the article by Marchioro and Pulvirenti (1993, 1994). These authors proved that the Euler dynamics is "similar" to the vortex dynamics in which the vortices are localized in very small regions, and the vortex intensities are the total vorticities associated to such small regions. In particular, let us consider a vorticity field with compact support on a family of ϵ-balls, that is,

$$\omega^\epsilon = \sum_{i=1}^{N}\omega_i^\epsilon$$

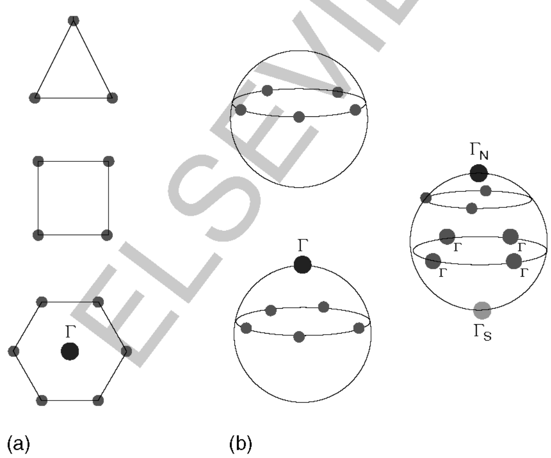

f0035 **Figure 7** Polygonal configuration of vortices: (a) planar configurations and (b) configurations of vortex rings on a sphere, with and without polar vortices.

f0040 **Figure 8** In the limit $\epsilon \to 0$, the dynamics of the center of vorticity of a vortex ϵ-ball is approximated by the dynamics of a point vortex.

with support of ω_i^ϵ contained in the ball of center x_i (independent of ϵ) and radius ϵ. Furthermore let us assume that

$$\int_{|\boldsymbol{r}-\boldsymbol{r}_i|\leq\epsilon} \omega_i^\epsilon \, \mathrm{d}\boldsymbol{r} = \Gamma_i$$

with the γ_i independent of ϵ. Then in the limit $\epsilon \to 0$ the dynamics of the center of vorticity $B_\epsilon(t) = \int \boldsymbol{r}\omega_\epsilon(\boldsymbol{r}, t)\, \mathrm{d}\boldsymbol{r}$, of a given ϵ-ball, "converges" to the motion of a single point vortex (see **Figure 8**). This result is important to illustrate as vortex systems provide both a useful heuristic tool in the analysis of the general properties of the solutions of Euler's equations (Poupaud 2002, Schochet 1995), and a useful starting point for the construction of practical algorithms for solving equations in specific situations. In particular, it provides a theoretical justification to the vortex method previously introduced by Carnevale *et al.* (1992). These authors constructed a numerical algorithm to study turbulence decaying in two dimensions. Their vortex method greatly simplifies fluid simulations as basically it relies on a discretization of the fluid into circular patches. The dynamics of patches is given by the centers of vorticity, which interact as a point-vortex system, endowed with a rule dictating as patches merge (see **Figure 9**).

s0015 Stability of a Vortex Ring

p0055 As mentioned in Introduction, the study of vortex relative equilibria has a long history. Kelvin showed that steadily rotating patterns of identical vortices arise as solutions of a variational problem in which the interaction energy (vortex Hamiltonian) is minimized subject to the constraint that the angular impulse be maintained (see Aref (2003). In 1883, while studying and modeling the atomic structure, J J Thomson investigated the linear stability of co-rotating point vortices in the plane. In particular, his interest was in configurations of identical vortices equally spaced along the circumference of a circle, that is, located at the vertices of a regular polygon (see **Figure 7**). He proved that for six of fewer vortices the polygonal configurations are stable, while for seven vortices – the Thomson heptagon – he erroneously concluded that the configuration is slightly unstable. It took more than a century to make some progresses on this problem. D G Dritschel (1985) succeeded in solving the heptagon mystery for what concerns its linear stability analysis, leaving open the nonlinear stability question: he proved that the Thomson heptagon is neutrally stable and that for eight or more vortices the corresponding polygonal configurations are linearly unstable. Later on in 1993, Polvani and Dritschel (1993) generalized the techniques used in Dritschel (1985) to study the linear stability of a "latitudinal" ring of point vortices on the sphere, as a function of the number N of vortices in the ring, and of the ring's co-latitude θ (see **Figure 10**). They proved that polygonal configurations are more unstable on the sphere than in the plane. In particular, they showed that at the pole, for $N < 7$ the configuration is stable, for $N = 7$ it is neutrally stable and for $N > 7$ it is unstable. By means of the energy momentum method (Marsden–Meyer–Weistein reduction), J E Marsden and S Pekarsky (1998) studied the nonlinear stability analysis for the integrable case of polygonal configurations of three vortices of arbitrary vorticities (Γ_1, Γ_2 and Γ_3) on the sphere, letting open the stability analysis for nonintegrable vortex systems ($N > 3$). In 1999 H E Cabral and D S Schmidt completed the linear and nonlinear stability

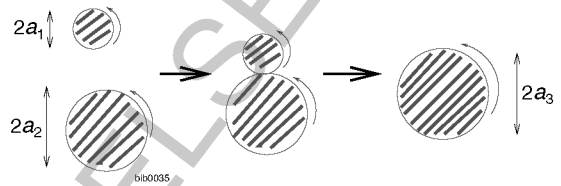

f0045 **Figure 9** In Carnevale *et al.* (1992) the fluid is modeled by a dilute vortex gas with density ρ and typical radius a. The dynamics is governed by the point-vortex dynamics of the disk centers, each disk corresponding to a point vortex of intensity $\Gamma = \pi\xi_{ext}a^2$, where ξ_{ext} plays the role of a vorticity density. Two vortices or radius a_1 and a_2 merge when their center-to-center distance is less or equal to the sum of their radii, $a_1 + a_1$. Then a new vortex is created and its radius a_3 is given by $a_3 = (a_1^4 + a_2^4)^{1/4}$.

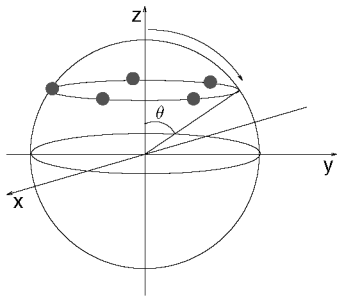

Figure 10 Latitudinal ring of vortices. Reproduced from *SIAM Journal of Applied Mathematics*. f0050 AU7

analysis at once for polygonal configurations in the plane. In 2003 Boatto and Cabral studied the nonlinear stability of a ring of vortices on the sphere, as a function of the number of vortices N and the ring colatitude θ. Boatto and Simó (2004) generalized the stability analysis to the case of a ring with polar vortices and of multiple rings, the key idea being, as we shall discuss in this section, the structure of the Hassian of the Hamiltonian.

p0060 *How to infer about linear and nonlinear stability of steadily rotating configurations?*

p0065 Let us restrict the discussion to a polygonal ring of identical vortices on a sphere as illustrated in **Figure 7** (Boatto and Cabral 2003, Boatto and Simó 2004). The reasoning is easily generalized for the planar case. The case of multiple rings is discussed in great detail in Boatto and Simó (2004). A polygonal ring is a relative equilibrium of coordinates $X(t) = (q_1(t), \ldots, q_N(t), p_1(t), \ldots, p_N(t))$, where

$$\begin{aligned} q_\alpha(t) &= \phi_\alpha(t) = \omega t + \phi_{o\alpha} \\ p_\alpha(t) &= p_o = \Gamma \cos\theta_o \quad \alpha = 1, \ldots, N \end{aligned} \qquad [18]$$

$\omega = (N-1)p_o/r_o^2, r_o = \sqrt{1 - p_o^2/\Gamma^2}, \phi_{o\alpha}$ and $\theta_{o\alpha} = \theta_o$ being the initial longitude and co-latitude of the αth vortex.

p0070 **Theorem 1** (Spherical case) (Boatto and Simó 2004). *The relative equilibrium* [18] *is (linearly and nonlinearly) stable if*

$$\begin{aligned} &-4(N-1)(11-N) + 24(N-1)r_o^2 \\ &\quad + 2N^2 + 1 + 3(-1)^N < 0 \end{aligned} \qquad [19]$$

and it is unstable if the inequality is reversed.

p0075 **Remarks**

(i) By Theorem 1 a vortex polygon, of N point vortices, is stable for $0° \le \theta_o \le \theta_o^*$ and $(180° - \theta_o^*) \le \theta_o \le 180°$, where $\theta_o^* = \arcsin(r_o^*)$ and

$$r_o^{*2} < \frac{7-N}{4} \quad \text{for } N \text{ odd}$$

$$r_o^{*2} < -\frac{N^2 - 8N + 8}{4(N-1)} \quad \text{for } N \text{ even}$$

where $r_o^* = \sin\theta_o^*$.

(ii) Theorem 1 includes at once the results of Thomson (1883), Dritschel (1985), and Polvani and Dritschel (1993) (and other authors which have been working in the area (Aref *et al.* 2003)). We recover the planar case by setting $r_o = 0$ in eqn [19], deducing that stability is guaranteed for $N < 7$.

p0080 To prove Theorem 1 it is useful to consider the Hamiltonian equations as in eqn [17]. The first step is to change of reference frame: view the dynamics in a frame co-rotating with the relative equilibrium configuration. In the co-rotating reference system, the Hamiltonian takes the form

$$\tilde{H} = H + \omega M$$

where M is the momentum of the system, and H and ω are, respectively, the Hamiltonian and the rotational frequency of the relative equilibrium in the original frame of reference. In the new reference frame, the relative equilibrium becomes an equilibrium, X^*, and the standard techniques can be used to study its stability.

p0085 To study linear stability, the relevant equation is

$$\frac{d\Delta X}{dt} = JS\Delta X \qquad [20]$$

where $X = X^* + \Delta X$, and S is the Hessian of $\tilde{H}$ evaluated at the equilibrium X^*. Then linear (or spectral) stability is deduced by studying the eigenvalues of the matrix JS (spectral stability). For nonlinear stability we make use of a sufficient stability criterion due to Dirichlet (1897) (Boatto and Cabral 2003): AU8

p0090 **Theorem 2** *Let X^* be an equilibrium of anautonomous system of ordinary differential equations*

$$\frac{dX}{dt} = f(X), \qquad \Omega \subset \mathbb{R}^{2N} \qquad [21]$$

that is, $f(X^*) = 0$. If there exists a positive (or negative) definite integral $\mathbf{F}$ of the system [21] *in a neighborhood of the equilibrium X^*, then X^* is stable.*

p0095 In our case the Hamiltonian itself is an integral of motion. Then by studying definiteness of its Hessian, S, evaluated at X^*, we infer minimal stability intervals in θ and N. Details are given in Boatto and Cabral (2003) and Boatto and Simó (2004). The proof is mainly based on the following considerations:

1. Since S is a symmetric matrix it is diagonalizable, that is, there exists an orthogonal matrix C such that $C^T S C = D$, where D is a diagonal matrix, $D = \mathrm{diag}(\lambda_1, \ldots, \lambda_N)$. Furthermore, the matrix C can be chosen to leave invariant the symplectic form (equivalently $J = C^T J C$). Then by the canonical change of variables $Y = C^T X$ eqn [20] becomes

$$\frac{d\Delta Y}{dt} = JD\Delta Y \qquad [22]$$

where $Y=(\tilde{q}_1,\ldots,\tilde{q}_N,\tilde{p}_1,\ldots,\tilde{p}_N)$ and $(\tilde{q}_j,\tilde{p}_j)$, $j=1,\ldots,N$, are pairs of conjugate variables. Equation [22] can be rewritten as

$$\frac{\mathrm{d}^2\Delta\tilde{q}_j}{\mathrm{d}t^2}=-\lambda_j\lambda_{j+N}\Delta\tilde{q}_j,\quad j=1,\ldots,N$$

2. When evaluated at the equilibrium X^*, the Hessian S takes the block structure

$$\tilde{S}=\begin{pmatrix}Q & O\\ O & P\end{pmatrix}$$

where the matrices Q and P are symmetric circulant matrices, that is, $(N\times N)$ matrices of the form

$$A=\begin{pmatrix}a_1 & a_2 & \ldots & a_N\\ a_N & a_1 & \ldots & a_{N-1}\\ \vdots & \vdots & \ddots & \vdots\\ a_2 & a_3 & \ldots & a_1\end{pmatrix} \qquad [23]$$

Circulant matrices are of special interest to us because we can easily compute their eigenvalues and eigenvectors for all N. In fact, it is immediate to show that:

p0100 **Lemma 3** *All circulant matrices* [23] *have eigenvalues*

$$\lambda_j=\sum_{k=1}^{N}a_k r_j^{k-1},\quad j=1,\ldots,N$$

and corresponding eigenvectors $v_j=(1,r_j,\ldots,r_j^{N-1})^{\mathrm{T}}, j=1,\ldots N$, *where* $r_j=\exp(2\pi(j-1)/N)$ *are solutions of* $r^N=1$.

s0020 **Passive Tracers in the Velocity Fields of N Point Vortices: The Restricted $(N+1)$-Vortex Problem**

p0105 The terminology "restricted $(N+1)$-vortex problem" is used in analogy with celestial mechanics literature, when one of the vorticities is taken to be AU25 zero. The zero-vorticity vortex does not effect the dynamics of the remaining N-vortices. For this reason, it is said to be passively advected by the flow of the remaining N-vortices and in the fluid mechanics' literature the terminology passive tracer is also employed. The tracer dynamics is given by the Hamiltonian equations [8]. Notice that in general the Hamiltonian Ψ is time dependent, through the vortex variables $\boldsymbol{r}_j, j=1,\ldots,N$, that is,

$$\Psi(\boldsymbol{r},t)=\Psi(\boldsymbol{r},\boldsymbol{r}_1(t),\ldots,\boldsymbol{r}_N(t))$$

and $(q,p)=(x,y)$ play the role of conjugate canonical variables. There is an extensive literature on the subject both from a theoretical (see, e.g., Boatto and Simó (2004) bib0085 and Newton (2001) bib0165) and an experimental (van Heijst 1993, Ottino 1990 bib0179) points of view. As discussed in the previous section, there are some vortex configurations, such as the polygonal ones, for which vortices undergo to a periodic circular motion. Then by viewing the dynamics in a reference frame co-rotating with the vortices the tracer Hamiltonian is manifestly time independent and, therefore, integrable – since it reduces to a Hamiltonian of one degree of freedom. In such an occurrence, tracer trajectories form a web of homoclinic and heteroclinic orbits. An interesting theoretical problem is to study how the tracer transport properties (i.e., existence of barriers to transport, diffusion etc.) are effected by perturbing the polygonal vortex configuration, that is, by introducing in Ψ a "genuine" time dependence (periodic, quasiperiodic, or chaotic) (see, e.g., Boatto and Pierrehumbert (1999), Rom-Kedar, Leonard and Wiggins (1990), Kuznetsov and Zaslavsky (2000), and Newton (2001) bib0165). Furthermore, in the lab experiments, color dyes, which monitor the flow velocity field, are often used as the experimental equivalent of tracer particles. In this contest we would like to stress the striking resemblance between theoretical particle trajectories, deduced from point vortex dynamics, and the actual dye visualizations observed by van Heijst and Flor for vortex dipoles in a stratified fluid (see **Figures 11** and **12**) (van Heijst 1993). Similarly, tripolar structures have been observed both in lab experiments (see **Figure 13**) and in nature (see **Figure 14**). Recently, the Danish group of Jansson–Haspang–Jensen–Hersen–Bohr has observed beautiful rotating polygons, such as squares and pentagons, on a fluid surface in the presence of a rotating cylinder (see **Figure 15**).

AU26 AU9

Point Vortex Motion with Boundaries s0025

p0110 In comparison with the extensive literature on point vortex motion in unbounded domains, the study of point vortex motion in the presence of walls is modest. There is, however, a general theory for such problems, and some recent new developments in this area has resulted in a versatile tool for analyzing point vortex motion with boundaries. Both Saffman and Newton (Newton 2001 bib0165) contain chapters on point vortex motion with boundaries, the latter also featuring a detailed bibliography. The reader is referred there for standard treatments; here, we focus on more recent developments of the mathematical theory.

The Method of Images s0030

p0115 When point vortices move around in bounded domains, it is clear that the motion is subject to the constraint that no fluid should penetrate any of

the boundary walls of the domain. If $\boldsymbol{n}$ denotes the local normal to the boundary walls, the boundary condition on the velocity field $\boldsymbol{u}$ is therefore $\boldsymbol{u} \cdot \boldsymbol{n} = 0$ everywhere on the walls. Another way to say the same thing is that all the walls must be streamlines so that the streamfunction, ψ say, must be constant on any boundary wall.

p0120 A classical approach to bounded vortex motion is the celebrated method of images – a rather special technique limited to cases where the domain of interest has certain geometrical symmetries so that an appropriate distribution of image vorticity can be ascertained, essentially by inspection. This image vorticity is placed in nonphysical regions of the plane in order to satisfy the boundary conditions that the walls act as impenetrable barriers for the flow.

p0125 The simplest example is the motion of a single vortex next to a straight plane wall of infinite extent. Suppose the wall is along $y = 0$ in an (x, y)-plane and that the fluid occupies the upper-half plane. If a circulation-Γ vortex is at the complex position $z_0 = x_0 + \mathrm{i}y_0$, the solution for the streamfunction is

$$\psi(z, \overline{z}) = -\frac{\Gamma}{2\pi} \log \left| \frac{z - z_0}{z - \overline{z_0}} \right| \qquad [24]$$

where $z = x + \mathrm{i}y$. This has a single logarithmic singularity in the upper-half plane at $z = z_0$

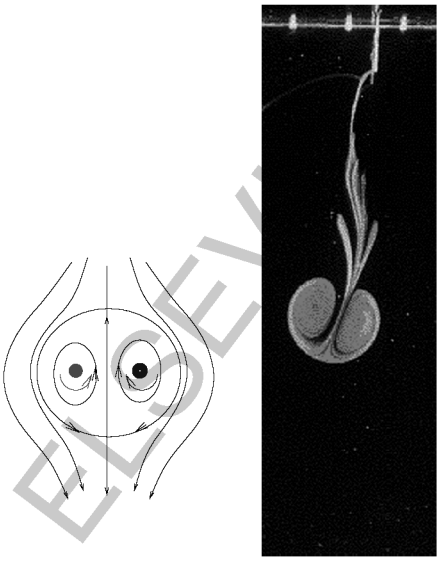

f0055 **Figure 11** Test-particle trajectories: on the left, theoretical trajectories, from the point-vortex model; on the right, a top view of a laboratory experiment in stratified flows. Reproduced from van Heijst GJF and Flor JB (1989) Dipole formation and collisions in a stratified fluid. *Nature* 340: 212–215, with AU10 permission from Nature Publishing Group.

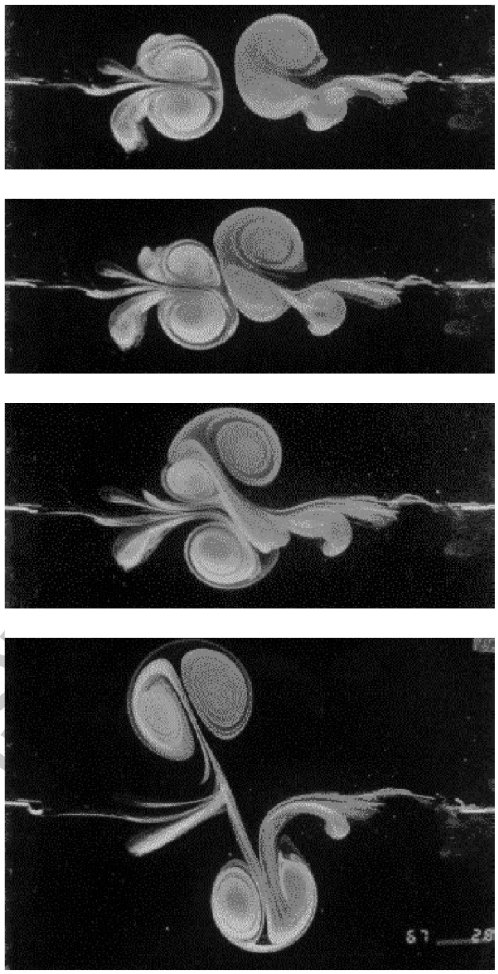

f0060 **Figure 12** A frontal collision of two dipoles as observed in a stratified fluid: after a so called "partner-exchange" two new dipoles are formed. Reproduced from van Heijst GJF and Flor JB (1989) Dipole formation and collisions in a stratified fluid. *Nature* 340: 212–215, with permission from Nature Publishing Group.

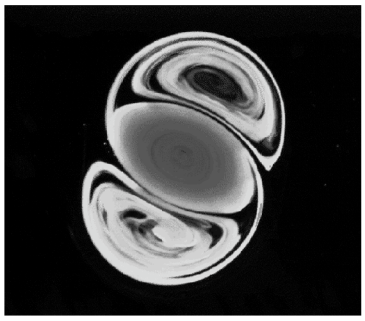

f0065 **Figure 13** A tripolar vortex structure as observed in a rotating stratified fluid. Reproduced from van Heijst GJF, Kloosterziel RC, and Williams CWM (1991) Laboratory experiments on the tripolar vortex in a rotating fluid. *Journal of Fluid Mechanics* 225: 301–331, with permission from Cambridge University Press.

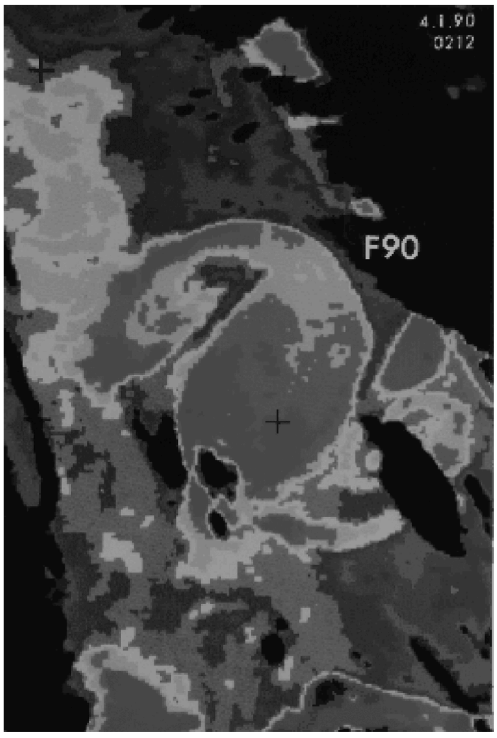

f0070 **Figure 14** Infrared image taken by NOAA11 satellite on January 4 1990 (0212 UT) shows a tripolar structure in the Bay of Biscay. The central part of the tripole measures about 50–70 km and rotates clockwise, whereas the two satellite vortices rotate anticlockwise. The dipoles persisted for a few days before it fell apart. Reproduced from Pingree RD and Le Cann B, Anticyclonic Eddy X91 in the Southern Bay of Biscay, *Journal of Geophysical Research*, 97: 14353–14362, May 1991 to February 1992. Copyright (1992) American Geophysical Union. Reproduced/modified by permission of American Geophysical Union. AU11

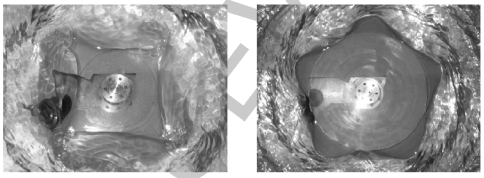

f0075 **Figure 15** The free surface of a rotating fluid will, due to the centrifugal force, be pressed radially outward. If the flow is driven by rotating the bottom plate, the axial symmetry can break spontaneously and the surface can take the shape of a rigidly rotating polygon. With water Jansson–Haspang–Jensen–Hersen–Bohr have observed polygons with up to six corners. The rotation speed of the polygons does not coincide with that of the plate, but it is often mode-locked, such that the polygon rotates by one corner for each complete rotation of the plate. Reproduced from Jansson TRN, Haspang M, Jensen KH, Hersen P, and Bohr T (2005) Rotating polygons on a fluid surface. *Preprint*, with permission from T Bohr.

(corresponding to the point vortex) and it is easily checked that $\psi = 0$ on $y = 0$. Therefore, no fluid penetrates the wall. Equation [24] can be written as

$$\psi(z,\overline{z}) = -\frac{\Gamma}{2\pi}\log|z - z_0| + \frac{\Gamma}{2\pi}\log|z - \overline{z_0}| \qquad [25]$$

which is the sum of the streamfunction due to a point vortex of circulation Γ at $z_0 = x_0 + \mathrm{i}y_0$ and another, one imagines, of circulation $-\Gamma$ at $\overline{z_0} = x_0 - \mathrm{i}y_0$. In this case, the image vortex distribution is simple: it is just the second vortex sitting at the reflected point in the wall. The method of images can be applied to flows in other regions bounded by straight line segments (e.g., wedge regions of various angles (Newton 2001)). bib0165

A variant of the method of images is the Milne–Thomson circle theorem relevant to planar flow around a circular cylinder. Given a complex potential $w(z)$ with the required singularities in the fluid region exterior to the cylinder, but failing to satisfy the boundary condition that the surface of the cylinder is a streamline, this theorem says that the correct potential $W(z)$ is p0130

$$W(z) = w(z) + \overline{w}(a^2/z) \qquad [26]$$

where a is the cylinder radius and $\overline{w}(z)$ is the conjugate function to $w(z)$. It is easy to verify that the imaginary part of $W(z)$, that is, the streamfunction, is zero on $|z| = a$. The second term, $\overline{w}(a^2/z)$, produces the required distribution of image vorticity inside the cylinder. A famous example is the Föppl vortex pair which is the simplest model of the trailing vortices shed in the wake of a circular aerofoil traveling at uniform speed.

Kirchhoff–Routh–Lin Theory s0035

The most important general mathematical tool for point vortex motion in bounded planar regions is the Hamiltonian approach associated with the names of Kirchhoff (1876) and Routh (1881), AU12 who developed the early theory. Lamb gives an account of their original work. It is now known that the problem of N-vortex motion in a simply connected domain is a Hamiltonian dynamical system. Moreover, the Hamiltonian has simple transformation properties when a given flow domain of interest is mapped conformally to another – a result originally due to Routh. A formula for the Hamiltonian can be built from knowledge of the instantaneous Green's function associated with motion of the point vortex in the simply connected domain D. In fact, [24] is precisely the relevant Green's function when D is the upper-half plane. p0135

p0140 Much later, in 1941, Lin (1941) extended these general results to the case of multiply connected fluid regions. To visualize such a region, think of a bounded region of the plane containing fluid but also a finite number of impenetrable islands whose boundaries act as barriers for the fluid motion. If the islands are infinitely thin, they can be thought of as straight wall segments immersed in the flow (see later examples). Lin (1941) showed that both the Hamiltonian structure, and the transformation properties of the Hamiltonian under conformal mapping, are preserved in the multiply connected case.

s0040 Lin's Special Green's Function

p0145 Since Lin's result subsumes the earlier simply connected studies, we now outline the key results as presented in Lin (1941). Consider a fluid region D, with outer boundary C_0 and M enclosed islands each having boundaries $\{C_j | j = 1, \ldots, M\}$. Lin introduced a special Green's function $G(x, y; x_0, y_0)$ satisfying the following properties:

1. the function

$$g(x, y; x_0, y_0) = -G(x, y; x_0, y_0) - \frac{1}{2\pi} \log r_0 \qquad [27]$$

is harmonic with respect to (x, y) throughout the region D including at the point (x_0, y_0). Here, $r_0 = \sqrt{(x - x_0)^2 + (y - y_0)^2}$;

2. if $\partial G / \partial n$ is the normal derivative of G on a curve then

$$G(x, y; x_0, y_0) = A_k, \quad \text{on } C_k, k = 1, \ldots, M$$
$$\oint_{C_k} \frac{\partial G}{\partial n} \, \mathrm{d}s = 0, \quad k = 1, \ldots, M \qquad [28]$$

where $\mathrm{d}s$ denotes an element of arc and $\{A_k\}$ are constants;

3. $G(x, y; x_0, y_0) = 0$ on C_0.

Flucher and Gustafsson (1997) refer to this G as the hydrodynamic Green's function. (In fact, it coincides with the modified Green's function arising in abstract potential theory – a function that is dual to the usual first-type Green's function that equals zero on all the domain boundaries.) On use of G, Lin established the following two key results:

p0150 **Theorem 4** *If N vortices of strengths $\{\Gamma_k | k = 1, \ldots, N\}$ are present in an incompressible fluid at the points $\{(x_k, y_k) | k = 1, \ldots, N\}$ in a general multiply connected region D bounded by fixed boundaries, the stream function of the fluid motion is given by*

$$\psi(x, y; x_k, y_k) = \psi_0(x, y) + \sum_{k=1}^{N} \Gamma_k G(x, y; x_k, y_k) \qquad [29]$$

where $\psi_0(x, y)$ is the streamfunction due to outside agencies and is independent of the point vortex positions.

p0155 **Theorem 5** For the motion of vortices of strengths $\{\Gamma_k | k = 1, \ldots, N\}$ in a general region D bounded by fixed boundaries, there exists a Kirchhoff–Routh function $H(\{x_k, y_k\})$, depending on the point vortex positions, such that

$$\Gamma_k \frac{\mathrm{d}x_k}{\mathrm{d}t} = \frac{\partial H}{\partial y_k}, \quad \Gamma_k \frac{\mathrm{d}y_k}{\mathrm{d}t} = -\frac{\partial H}{\partial x_k} \qquad [30]$$

where $H(\{x_k, y_k\})$ is given by

$$H(\{x_k, y_k\}) = \sum_{k=1}^{N} \Gamma_k \psi_0(x_k, y_k) + \sum_{\substack{k_1, k_2 - 1 \\ k_1 > k_2}}^{N} \Gamma_{k_1} \Gamma_{k_2} G(x_{k_1}, y_{k_1}; x_{k_2}, y_{k_2}) - \frac{1}{2} \sum_{k=1}^{N} \Gamma_k^2 g(x_k, y_k; x_k, y_k) \qquad [31]$$

In rescaled coordinates $(x_k, \Gamma_k y_k)$, [30] is a Hamiltonian system in canonical form. For historical reasons, H is often called the Kirchhoff–Routh path function. Analyzing the separate contributions to the path function [31] is instructive: the first term is the contribution from flows imposed from outside (e.g., background flows and round-island circulations), the second term is the "free-space" contribution (it is the relevant Hamiltonian when no boundaries are present) while the third term encodes the effect of the boundary walls (or, the effect of the "image vorticity" distribution discussed earlier).

p0160 Lin (1941) went on to show that, with the Hamiltonian in some D given by H in [31], the Hamiltonian relevant to vortex motion in another domain obtained from D by a conformal mapping $z(\zeta)$ consists of [31] with some simple extra additive contributions dependent only on the derivative of the map $z(\zeta)$ evaluated at the point vortex positions.

p0165 Flucher and Gustafsson (1997) also introduce the Robin function $\mathcal{R}(x_0, y_0)$ defined as the regular part of the above hydrodynamic Green's function evaluated at the point vortex. Indeed, $\mathcal{R}(x_0, y_0) \equiv g(x_0, y_0; x_0, y_0)$, where g is defined in [27]. An interesting fact is that, for single-vortex motion in a simply connected domain, $\mathcal{R}(x_0, y_0)$ satisfies the quasilinear elliptic Liouville equation everywhere in

D with the boundary condition that it becomes infinite everywhere on the boundary of D.

p0170 By combining the Kirchhoff–Routh theory with conformal mapping theory, many interesting problems can be studied. What happens, for example, if there is a gap in the wall of **Figure 16**? In recent work, Johnson and McDonald (2005) show that if the vortex starts off, far from the gap, at a distance of less than half the gap width from the wall, then it will eventually penetrate the gap. Otherwise, it will dip towards the gap but not go through it. The trajectories are shown in **Figure 17**.

p0175 Unfortunately, Lin did not provide any explicit analytical expressions for G in the multiply connected case. This has limited the applicability of his theory beyond fluid regions that are anything other than simply and doubly connected. Recently, however, Lin's theory has recently been brought to implementational fruition by Crowdy and Marshall (2005), who, up to conformal mapping, have derived explicit formulas for the hydrodynamic Green's function in multiply connected fluid regions of arbitrary finite connectivity. Their approach makes use of elements of classical function theory dating back to the work of Poincare, Schottky, and Klein (among others). This allows new problems involving bounded vortex motion to be tackled. For example, the motion of a single vortex around multiple circular islands has been studied in Crowdy and Marshall (2005), thereby extending recent work on the two-island problem (Johnson and McDonald 2005). If the wall in **Figure 17** happens to have two (or more) gaps, then the fluid region is multiply connected. The two-gap (doubly connected) case was recently solved by Johnson and McDonald (2005) using Schwarz–Christoffel maps combined with elements of elliptic function theory (see **Figure 18**). Crowdy and Marshall have solved the problem of an arbitrary number of gaps in a wall by exploiting the new general theory presented in Crowdy and Marshall (2005) (and related works by the authors). The case of a wall with three gaps represents a triply connected fluid region and the critical vortex trajectory is plotted in **Figure 19**.

p0180 Point vortex motion in bounded domains on the surface of a sphere has received scant attention in

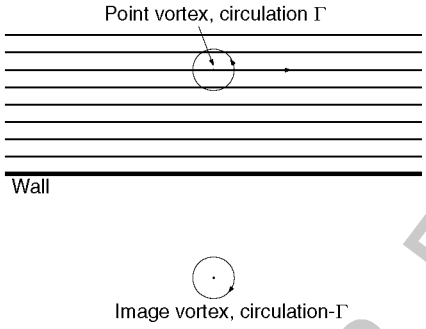

f0080 **Figure 16** The motion of a point vortex near an infinite straight wall. The vortex moves, at constant speed, maintaining a constant distance from the wall. Other possible trajectories are shown; they are all straight lines parallel to the wall. The motion can be thought of as being induced by an opposite-circulation "image" vortex at the reflected point in the wall.

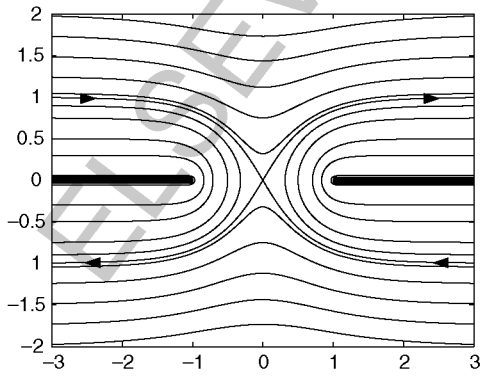

f0085 **Figure 17** Distribution of point vortex trajectories near a wall with a single gap of length 2. There is a critical trajectory which, far from the gap, is unit distance from the wall.

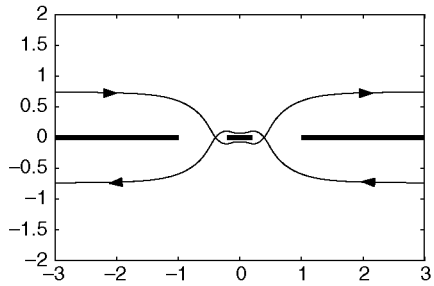

f0090 **Figure 18** The critical trajectory when there are two symmetric gaps in a wall. The fluid region is now doubly connected. This problem is solved in Johnson and McDonald (2005) and Crowdy and Marshall (2005).

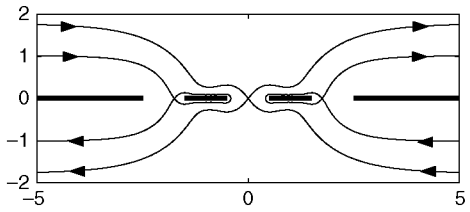

f0095 **Figure 19** The critical vortex trajectories when there are three gaps in the wall. This time the fluid region is triply connected. This problem is solved in Crowdy and Marshall (2005) using the general methods in Crowdy and Marshall (2005).

AU13 the literature, although b0165 Kidambi and Newton (2000) and Newton (2001) have recently made a contribution. Such paradigms are clearly relevant to planetary-scale oceanographic flows in which oceanic eddies interact with topography such as ridges and land masses and deserve further study.

Further Reading

b0005 Albouy A (1996) The symmetric central configurations of four equal masses. *Contemporary Mathematics* 198: 131–135.

b0010 Aref H, Newton PK, Stremler MA, Tokieda T, and Vainchtein DL
AU14 (2003) Vortex crystals. *Advances in Applied Mathematics* 39.

b0015 Aref H and Stremler MA (1999) Four-vortex motion with zero total circulation and impulse. *Physics of Fluids* 11(12): 3704–3715.

b0020 Ball WWR (1940) *A Short Account of the History of Mathe-*
AU15 *matics*, 12th edn. MacMillan.

b0025 Boatto S and Cabral HE (2003) Nonlinear stability of a latitudinal ring of point vortices on a non-rotating sphere. *SIAM Journal of Applied Mathematics* 64: 216–230.

b0030 Boatto S and Simó C (2004) Stability of latitudinal vortex rings
AU16 with polar vortices. *Preprint*.

b0035 Carnevale GF, McWilliams JC, Pomeau Y, Weiss JB, and Young WR (1992) Rates, pathways, and end states of nonlinear evolution in decaying two-dimensional. *Physics of Fluids A* 4(6): 1314–1316.

b0040 Carnevale GF, McWilliams JC, Pomeau Y, Weiss JB, and Young WR (1991) Evolution of vortex statistics in two-dimensional turbulence. *Physical Review Letters* 66(21): 2735–2737.

b0045 Castilla MSAC, Moauro V, Negrini P, and Oliva WM (1993) The four positive vortices problem – regions of chaotic behavior and non-integrability. *Annales de l'Institut Henri Poincaré –*
AU17 *Phys. Theor* 59(1): 99–115.

b0050 Crowdy DG and Marshall JS (2005) Analytical formulae for the Kirchhoff–Routh path function in multiply connected domains. *Proceedings of the Royal Society A* 461: 2477–2501.

b0055 Crowdy DG and Marshall JS (2005) The motion of a point vortex around multiple circular islands. *Physics of Fluids* 17: 560–602.

b0060 Dritschel DG (1985) The stability and energetics of co-rotating uniform vortices. *Journal of Fluid Mechanics* 157: 95–134.

b0065 Flucher M and Gustafsson B (1997) *Vortex Motion in Two Dimensional Hydrodynamics*. Royal Institute of Technology Report No. TRITA-MAT-1997-MA-02.

b0070 Glass K (2000) Symmetry and bifurcations of planar configurations of the *N*-body and other problems. *Dynamics and Stability of Systems* 15(2): 59–73.

b0075 van Heijst GJF and Flor JB (1989) Dipole formation and collisions in a stratified fluid. *Nature* 340: 212–215.

b0080 van Heijst GJF, Kloosterziel RC, and Williams CWM (1991) Laboratory experiments on the tripolar vortex in a rotating fluid. *Journal of Fluid Mechanics* 225: 301–331.

b0085 van Heijst GJF (1993) Self-organization of two-dimensional flows. *Nederlands Tijdschrift voor Natuurkunde* 59: 321–325 (http://www.fluid.tue.nl).

b0090 von Helmholtz H (1858) On the integrals of the hydrodynamical equations which express vortex motion. *Philosophical Magazine* 4(33): 485–512.

Jansson TRN, Haspang M, Jensen KH, Hersen P, and Bohr T b0095
(2005) Rotating polygons on a fluid surface. *Preprint*.

Johnson ER and McDonald NR (2005) Vortices near barriers b0100
with multiple gaps. *Journal of Fluid Mechanics* 531: 335–358.

Kimura Y (1999) Vortex motion on surfaces with constant b0105
curvature. *Proceedings of the Royal Society of London A* 455: 245–259.

Koiller J and Carvalho SP (1989) Non-integrability of the 4- b0110
vortex system: analytical proof. *Communications in Mathematical Physics* 120(4): 643–652.

Lin CC (1941) On the motion of vortices in two dimensions. I. b0115
Existence of the Kirchhoff–Routh function. *Proceedings of the National Academy of Sciences* 27(12): 570–575.

Lin CC (1941) On the motion of vortices in two dimensions. II. b0120
Some further investigations on the Kirchhoff–Routh function. *Proceedings of the National Academy Sciences* 27(12): 575–577.

Marchioro C and Pulvirenti M (1993) Vortices and localization in b0125
Euler flows. *Communications in Mathematical Physics* 154: 49–61.

Marchioro C and Pulvirenti M (1994) *Mathematical Theory of* b0130
Incompressible Non-viscous Fluids vol. 96 AMS vol. 96. New York: Springer.

Mayer AM (1878) *American Journal of Science and Arts* 15: b0135
276–277. AU18 AU19

Mayer AM (1878) *Nature* 17: 487–488. b0140 AU20

Mayer AM (1878) *Scientific American* 2045–2047. b0145 AU21

Mayer AM (1878) *American Journal of Science* 16: 247–256. b0150 AU22

Mayer AM (1878) *Philosophical Magazine* 7: 98–108. b0155 AU23

Montaldi J, Soulière A, and Tokieda T (2002) Vortex dyanmics b0160
on a cylinder. *SIAM Journal of Applied Dynamical Systems* 2(3): 417–430.

Newton PK (2001) *The N-Vortex Problem. Analytical Techni-* b0165
ques. New York: Springer.

Ottino JM (1990) *The Kinematics of Mixing: Stretching, Chaos* b0170
and Transport. Cambridge: Cambridge University Press.

Pingree RD and Le Cann B (1992) Anticyctonic Eddy X91 in the b0175
Southern Bay of Biscay. *Journal of Geophysical Research* 97: 14353–14362.

Polvani LM and Dritschel DG (1993) Wave and vortex dynamics b0180
on the surface of a sphere. *Journal of Fluid Mechanics* 255: 35–64.

Poupaud F (2002) Diagonal defect measures, adhesion dynamics b0185
and Euler equation. *Methods and Applications of Analysis* 9(4): 533–562.

Schochet S (1995) The weak vorticity formulation of the 2-D b0190
Euler equations and concentration-cancellation. *Communications in Partial Differential Equations* 20(5&6): 1077–1104.

Thomson W (1867) On vortex atoms. *Proceedings of the Royal* b0195
Society of Edinburgh 6: 94–105.

Thomson JJ (1883) *A Treatise on the Motion of Vortex Rings*. b0200
New York: Macmillian. AU24

Thomson JJ (1904) *Electricity and Matter*. Westmister Archibald b0205
Constable.

Yarmchuk EJ, Gordon MJV, and Packard RE (1979) Observation b0210
of stationary vortices arrays in rotating superfluid Helium. *Physical Review Letters* 43(3): 214–217.

Ziglin SL (1982) Quasi-periodic motions of vortex systems. b0215
Physica D 4: 261–269 (addedum to K M Khanin).